

Stable mass transfer can explain massive binary black hole mergers with a high spin component

YONG SHAO^{1,2} AND XIANG-DONG LI^{1,2}

¹*Department of Astronomy, Nanjing University, Nanjing 210023, People's Republic of China; shaoyong@nju.edu.cn*

²*Key laboratory of Modern Astronomy and Astrophysics (Nanjing University), Ministry of Education, Nanjing 210023, People's Republic of China; lixd@nju.edu.cn*

ABSTRACT

Recent gravitational wave observations showed that binary black hole (BBH) mergers with massive components are more likely to have high effective spins. In the model of isolated binary evolution, BH spins mainly originate from the angular momenta of the collapsing cores before BH formation. Both observations and theories indicate that BHs tend to possess relatively low spins, the origin of fast-spinning BHs remains a puzzle. We investigate an alternative process that stable Case A mass transfer may significantly increase BH spins during the evolution of massive BH binaries. We present detailed binary evolution calculations and find that this process can explain observed high spins of some massive BBH mergers under the assumption of mildly super-Eddington accretion.

Keywords: Gravitational waves – Compact binary stars – Black holes – Stellar evolution

1. INTRODUCTION

Since the discovery of the first gravitational wave source GW150914 (Abbott et al. 2016), there are about 90 binary black hole (BBH) mergers reported to date (Abbott et al. 2019, 2021a,b; Nitz et al. 2021). A number of formation channels have been put forward to explain the origin of BBH mergers (see Mandel & Broekgaarden 2022, for a review). In the isolated binary evolution channel, compact BH binaries are formed either through common envelope evolution (e.g., Tutukov & Yungelson 1993; Lipunov et al. 1997; Voss & Tauris 2003; Belczynski et al. 2016; Eldridge & Stanway 2016; Stevenson et al. 2017; Khokhlov et al. 2018; Kruckow et al. 2018; Mapelli & Giacobbo 2018; Giacobbo & Mapelli 2018; Spera et al. 2019; Breivik et al. 2020; Zevin et al. 2020; Broekgaarden et al. 2021) or through stable mass transfer between the BH and its companion (e.g., van den Heuvel et al. 2017; Neijssel et al. 2019; Bavera et al. 2021; Olejak et al. 2021; Shao & Li 2021; Gallegos-Garcia et al. 2021). Alternatively, merging BHs can be formed via dynamical interactions in globular clusters (Downing et al. 2010; Rodriguez et al. 2016; Askar et al. 2017; Perna et al. 2019; Kremer et al. 2020) or young stellar clusters (Ziosi et al. 2014; Di Carlo et al. 2019; Santoliquido et al. 2020; Rastello et al. 2020; Mapelli et al. 2022). Other formation channels involve isolated multiple systems (Silsbee & Tremaine 2017; Liu & Lai 2018; Hoang et al. 2018; Fragione & Loeb 2019), the chemically homogeneous evolution for rapidly rotating stars (Mandel & de Mink 2016; de Mink & Mandel 2016; Marchant et al. 2016),

the disk of active galactic nuclei (Antonini & Rasio 2016; Stone et al. 2017; McKernan et al. 2018), as well as the evolution of Population III binary stars (Kinugawa et al. 2014; Tanikawa et al. 2021).

Gravitational wave observations (Abbott et al. 2021b) indicate that the majority of BBH mergers have low effective spin parameters

$$\chi_{\text{eff}} = \frac{M_{1,\text{BH}} a_{1,\text{BH}} \cos \theta_1 + M_{2,\text{BH}} a_{2,\text{BH}} \cos \theta_2}{M_{1,\text{BH}} + M_{2,\text{BH}}}, \quad (1)$$

with $\chi_{\text{eff}} \sim 0$. Here $M_{1,\text{BH}}$ and $M_{2,\text{BH}}$ are the masses of both components, $a_{1,\text{BH}}$ and $a_{2,\text{BH}}$ the dimensionless BH spin magnitudes, and θ_1 and θ_2 the angles made by each component spin relative to the binary orbital angular momentum. For other minority mergers, there is a feature that the systems with the most extreme spins have heavier masses (Abbott et al. 2021b, see also Figure 3). The distribution of BH spin orientations offers vital clues on the evolutionary pathways that produce merging BBHs (e.g., Roulet et al. 2021; Galaudage et al. 2021; Callister et al. 2021; Stevenson 2022). BBH mergers formed from isolated binary evolution tend to have spins preferentially aligned with their orbital angular momenta, while dynamically assembled systems are expected to possess isotropically oriented spins. Recent analyses on the distribution of BH spin orientations supported the hypothesis that all merging systems originate from the isolated binary evolution channel (Galaudage et al. 2021). In this channel, tidal interaction between both components of BBH's progenitor systems is the

most promising mechanism for the origin of BH spins, which is effective for the binaries with very close orbits (e.g., Qin et al. 2018; Belczynski et al. 2020; Bavera et al. 2020, 2021; Olejak & Belczynski 2021; Fuller & Lu 2022). More recently, van Son et al. (2021) suggested that the stable mass-transfer channel mainly produces BBH mergers with component masses above $30M_{\odot}$, while the common-envelope channel predominately forms systems with component masses below about $30M_{\odot}$. Thus, we propose that the observed high effective spins of massive BBH mergers may relate to the process of mass accretion onto BHs during previous stable mass-transfer phases. It is worth to note that tidal interaction (e.g., Olejak & Belczynski 2021) may spin up only the second-formed BH (with rare case of equal mass ratios when both BHs may be spun up). In case of our study, the first-born BH is a subject of spin-up which is important in context of e.g. X-ray binary observations (Podsiadlowski et al. 2003).

In this paper, we investigate the influence of Case A mass transfer on the evolution of the accreting BHs and show that likely accounts for BBH systems with a fast-spinning component. Previous population synthesis studies did not predict the formation of high spin BHs via mass accretion because this process was thought to occur vary rapidly (e.g., Bavera et al. 2021; Zevin & Bavera 2022) and BHs can hardly accrete any material during the evolution (see e.g., van Son et al. 2020, as an exception). However, more detailed investigations indicate efficient spin up of BHs by stable mass accretion in X-ray binaries (King & Kolb 1999; Podsiadlowski et al. 2003; Fragos & McClintock 2015; Shao & Li 2020). Evolution of close massive primordial binaries has been well studied over past decades (e.g., Pols 1994; Wellstein 2001; Shao & Li 2016). If the initial orbital period is around a few days, Roche lobe overflow starts with Case A mass transfer when the donor star still undergoes core hydrogen burning. The Case A mass transfer episode usually consists of two phases. The first is a rapid phase during which the mass ratio of binary components is more or less reversed. The rapid mass-transfer phase happens roughly on the thermal timescale of the donor star. This phase is followed by a slower mass-transfer phase which occurs on the nuclear-expansion timescale of the donor star. Compared to the rapid phase, mass transfer usually takes place at a rate several orders of magnitude smaller in the slow phase. Since the population synthesis method simulates mass transfer via Roche lobe overflow in a rather crude way, here we perform detailed binary evolution calculations to examine the possible influence of mass accretion on the BH spins.

2. METHOD

We use the stellar evolution code Modules for Experiments in Stellar Astrophysics *MESA* (version 10398, Paxton et al. 2011, 2013, 2015, 2018, 2019) to model the evolution of binary systems containing a donor star of mass $20 - 100M_{\odot}$ (by a step of $20M_{\odot}$) and an accreting BH of mass $10 - 30M_{\odot}$ (by a step of $10M_{\odot}$). The initial binaries are set to have circular orbits, and the orbital periods increase from 1 day to 100 days by a logarithmic step of 0.1. The BH is regarded as a point mass, and the donor star begins its evolution from zero-age main sequence. All the models are calculated at solar metallicity ($Z = 0.02$) and a subsolar metallicity ($Z = 0.001$). We refer to Shao & Li (2021) for a detailed description of the input parameters in the code.

For spherically symmetric accretion, the mass increase onto a BH of mass M_1 is constrained by the Eddington limit

$$\dot{M}_{\text{Edd}} = \frac{4\pi GM_1}{\eta\kappa c} \simeq 7.8 \times 10^{-7} \left(\frac{M_1}{30M_{\odot}} \right) M_{\odot}\text{yr}^{-1}, \quad (2)$$

where G is the gravitational constant, κ is the radiative opacity which taken to be $0.2(1 + X)\text{cm}^2\text{g}^{-1}$ for a composition with hydrogen mass fraction X , c is the speed of light in vacuum, and η is the efficiency of the BH in converting rest mass into radiative energy (see also Podsiadlowski et al. 2003). This efficiency can be approximately given by

$$\eta = 1 - \sqrt{1 - \left(\frac{M_1}{3M_{1i}} \right)^2} \quad (3)$$

for $M_1 < \sqrt{6}M_{1i}$, where M_{1i} is the initial mass of the BH (Bardeen 1970). Note that $\eta \sim 0.1$ always holds in our calculations. When the BH accretes mass and angular momentum, its spin magnitude a_1 evolves according to

$$a_1 = \left(\frac{2}{3} \right)^{1/2} \frac{M_{1i}}{M_1} \left\{ 4 - \left[18 \left(\frac{M_{1i}}{M_1} \right)^2 - 2 \right]^{1/2} \right\} \quad (4)$$

for $M_1 < \sqrt{6}M_{1i}$ (Thorne 1974).

For radiation pressure dominated accretion disks, Begelman (2002) found that super-Eddington accretion rates of a factor of 10 can be achieved due to the development of a photon-bubble instability (see also Ruszkowski & Begelman 2003). This instability results in a large part of the disk volume being constituted of tenuous plasma, while the bulk of the mass is constrained in high-density regions. The photons can diffuse out of the disk mostly through the tenuous regions, therefore enhancing the Eddington limit. In our calculations, we

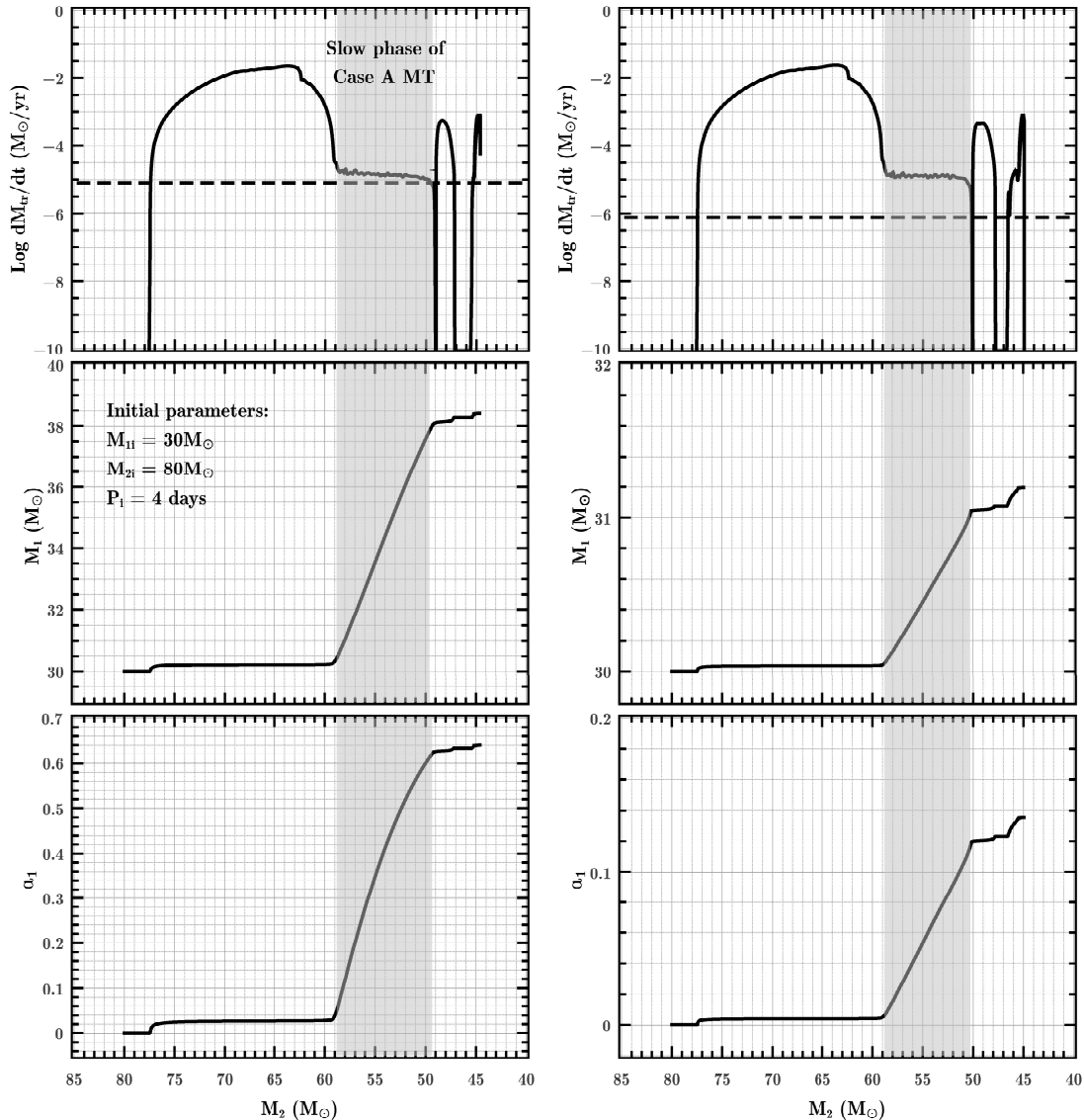


Figure 1. Evolutionary tracks of a binary initially containing a $30M_{\odot}$ BH and a $80M_{\odot}$ donor in a 4-day orbit. The top, middle, and bottom panels correspond to the mass transfer rate \dot{M}_{tr} , the BH mass M_1 , and its spin magnitude a_1 , respectively, as a function of the donor mass M_2 . The left and right panels correspond to the BH accretion rate being limited by $\dot{\mathcal{M}}_{\text{Edd}}$ and \dot{M}_{Edd} during the evolution, respectively. The two dashed lines mark the positions of $\dot{\mathcal{M}}_{\text{Edd}}$ and \dot{M}_{Edd} for a $30M_{\odot}$ accreting BH. The gray rectangle in each panel denotes the binary being in the slow phase of Case A mass transfer.

relax the Eddington accretion rate to be

$$\dot{\mathcal{M}}_{\text{Edd}} = 10\dot{M}_{\text{Edd}} \simeq 7.8 \times 10^{-6} \left(\frac{M_1}{30M_{\odot}} \right) M_{\odot}\text{yr}^{-1} \quad (5)$$

(see also Rappaport et al. 2005). Each binary evolution calculation is terminated if the donor star has developed an iron core or the time steps exceed 30,000. We assume that the donor eventually collapses into a BH without any mass loss and kick, and the new born BH possesses negligible spin (i.e. $a_{2,\text{BH}} \sim 0$, Belczynski et al. 2020). For simplicity, the spin of the accreting BH is assumed to be aligned with the orbital angular momentum of the

binary system ($\theta_1 = 0^\circ$). We follow Peters (1964) to treat the subsequent orbital evolution of the BBH system that is controlled by gravitational wave radiation. If the BBH system evolves to merge within a Hubble time, the effective spin parameter can be estimated to be

$$\chi_{\text{eff}} \simeq \frac{M_{1,\text{BH}}}{M_{1,\text{BH}} + M_{2,\text{BH}}} a_{1,\text{BH}}. \quad (6)$$

3. RESULTS

Figure 1 shows the evolution of a binary initially containing a $30M_{\odot}$ BH and a $80M_{\odot}$ zero-age main-sequence

companion in a 4-day orbit. The metallicity of the initial companion is taken to be 0.001. The left and right panels correspond to the cases that the BH accretion rate is limited by \dot{M}_{Edd} and \dot{M}_{Edd} , respectively. When the companion star evolves to fill its Roche lobe, about $2M_{\odot}$ hydrogen envelope has been blown away due to a stellar wind. At this moment, the donor star is still on main sequence (Case A evolution). A phase of rapid mass transfer proceeds at a rate up to $10^{-2}M_{\odot}\text{yr}^{-1}$, during which $\sim 20M_{\odot}$ material is stripped from the donor star but the BH hardly accretes. Subsequently, the system experiences a slow mass-transfer phase that is driven by the nuclear-expansion of the donor star. During this phase, the mass transfer occurs at a rate of the order $10^{-5}M_{\odot}\text{yr}^{-1}$. In the \dot{M}_{Edd} case, the BH can accrete $\sim 8M_{\odot}$ material and reach a spin of ~ 0.6 . After the Case A evolution, the system undergoes two other relatively short mass-transfer phases. Assuming that the donor directly collapses into a BH, we finally have a BBH system ($M_{1,\text{BH}} \sim 38M_{\odot}$ and $M_{2,\text{BH}} \sim 45M_{\odot}$) with an orbital period of ~ 1.8 days. About 0.6 Gyr later, this BBH is expected to merge with $\chi_{\text{eff}} \sim 0.3$. It is obvious that the slow Case A mass-transfer phase is key to produce the high BH spin. This phase can last for around 0.7 Myr (see Figure 2). For comparison, in the \dot{M}_{Edd} case, the BH can totally accrete $\sim 1M_{\odot}$ material with a relatively low spin of ~ 0.1 , and the BBH merger has an effective spin of $\chi_{\text{eff}} \sim 0.06$.

In Figure 3, we present the relations of $M_{1,\text{BH}}$ versus $M_{2,\text{BH}}$ (top panels) and $M_{1,\text{BH}}$ versus χ_{eff} (bottom panels) for the BBH systems that can merge within a Hubble time. The left and right panels correspond to the cases that the BH accretion rate is constrained by \dot{M}_{Edd} and \dot{M}_{Edd} (for comparison), respectively. In each panel, the black and blue triangles correspond to the calculated results with $Z = 0.001$ and $Z = 0.02$, respectively. Also plotted are the BBH mergers with high χ_{eff} measurements from gravitational wave observations (Abbott et al. 2021b). The initial binaries with a $20M_{\odot}$ donor always evolve to produce wide BBHs that cannot merge within a Hubble time, so the triangle symbols do not appear to show these BBHs in this figure. We can see that the calculated parameter distributions in the \dot{M}_{Edd} case can roughly match the observations. In this case, the χ_{eff} distribution is predicted to vary in a wide range of $\sim 0 - 0.6$. The source GW190517 seems to be an outlier with relatively light component masses ($25.3^{+7.0}_{-7.3}M_{\odot}$ and $37.4^{+11.7}_{-7.6}M_{\odot}$) and large effective spin ($\chi_{\text{eff}} = 0.52^{+0.19}_{-0.19}$). We note that mass transfer in the progenitor binaries with a $30M_{\odot}$ BH and a $40M_{\odot}$ companion can eventually lead to the reversal of component masses (i.e. $M_{1,\text{BH}} > M_{2,\text{BH}}$). For one mass-reversed system, its

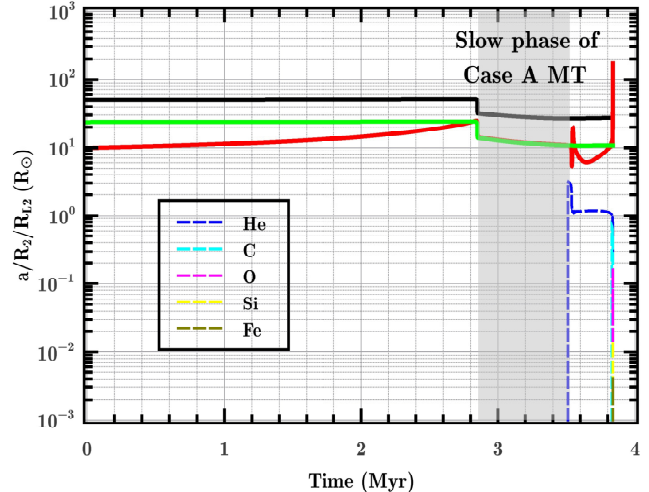


Figure 2. Evolution of the donor radius R_2 (the red curve), its Roche lobe radius R_{L2} (the green curve) and the binary separation a (the black curve) as a function of time for a binary initially containing a $30M_{\odot}$ BH and a $80M_{\odot}$ donor in a 4-day orbit. The five dashed curves represent the radii of donor’s cores. The gray rectangle denotes the binary being in the slow phase of Case A mass transfer. At the time of ~ 3.83 Myr, the stripped donor rapidly expands with radius beyond the size of the binary separation. At this moment, the donor has formed a $\sim 43M_{\odot}$ core surrounded by a $\sim 2M_{\odot}$ envelope at an advanced evolutionary stage. This system may have not enough time to develop a common-envelope phase before the donor collapses. Even if common-envelope evolution indeed occurs, this binary can survive the spiral-in phase for $\alpha_{\text{CE}}\lambda \gtrsim 0.03$ (using Equations (1) and (2) in Shao & Li 2014).

calculated parameters ($M_{2,\text{BH}} \sim 18M_{\odot}$, $M_{1,\text{BH}} \sim 42M_{\odot}$ and $\chi_{\text{eff}} \sim 0.53$) are consistent with the measured values of GW190517 within errors. In the \dot{M}_{Edd} case, most of calculated BBH mergers have the effective spins of $\lesssim 0.2$, which are obviously lower than observed.

Figure 4 shows the relations between the effective spin parameters χ_{eff} of calculated BBH mergers and the initial orbital periods P_1 of the progenitor binaries we evolved, assuming the BH accretion rate to be limited by \dot{M}_{Edd} . There is a tendency that the progenitor systems with shorter orbital periods are more likely to produce the BBH mergers with higher effective spins. The binaries with $P_1 \lesssim 5 - 10$ days experienced relatively slow mass-transfer phases, leading to the formation of the BBH mergers with $\chi_{\text{eff}} \gtrsim 0.1 - 0.2$. Based on our calculations, all progenitor systems with $M_{2i}/M_{1i} \leq 1$ evolve to be wide BBHs that cannot merge within a Hubble time. On the other hand, the binaries with $M_{2i}/M_{1i} > 3$ and $P_1 \lesssim 5 - 10$ days underwent dynamically unstable mass transfer (Shao & Li 2021) and probably led to bi-

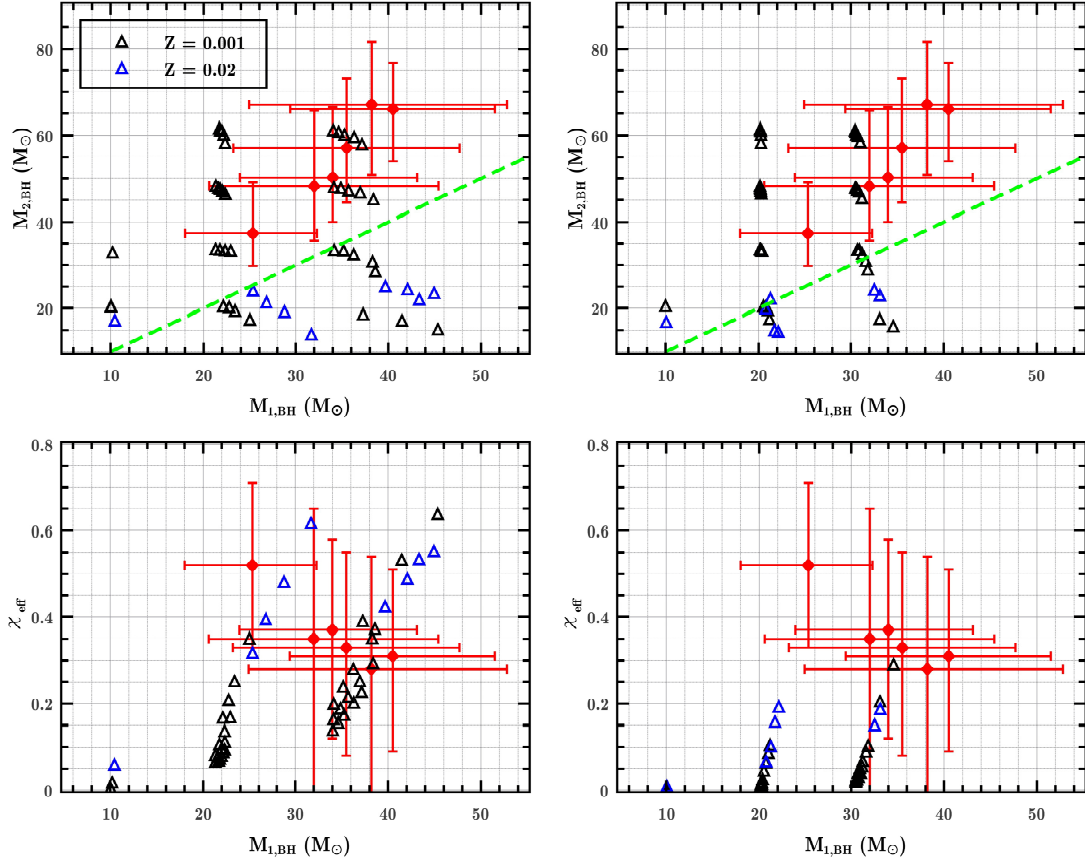


Figure 3. Relations of $M_{1,\text{BH}}$ versus $M_{2,\text{BH}}$ (top panels) and $M_{1,\text{BH}}$ versus χ_{eff} (bottom panels) for calculated BBH mergers. The black and blue triangles correspond to the results with $Z = 0.001$ and $Z = 0.02$, respectively. The red diamonds represent six observed systems with high χ_{eff} measurements, corresponding to the sources GW170729, GW190517, GW190519, GW190620, GW190706, and GW190805 (Abbott et al. 2021b). The left and right panels correspond to the cases that the BH accretion rate is limited by \dot{M}_{Edd} and \dot{M}_{Edd} during the progenitor evolution, respectively. The green dashed line shows the relation of $M_{1,\text{BH}} = M_{2,\text{BH}}$.

nary mergers involving a nondegenerate star and a BH. Hence the progenitor binaries with $1 \lesssim M_{2i}/M_{1i} \lesssim 3$ and $P_i \lesssim 5 - 10$ days mainly contribute the descendent BBH mergers with high effective spins. We note that some known BH binaries resemble the configurations of such progenitor systems. For example, Cgy X-1 contains a BH of mass $21.2 \pm 2.2 M_{\odot}$ and a donor star of mass $40.6^{+7.7}_{-7.1} M_{\odot}$ in a 5.6-day orbit (Miller-Jones et al. 2021). M33 X-7 hosts a $15.65 \pm 1.45 M_{\odot}$ BH and a $70.0 \pm 6.9 M_{\odot}$ donor orbiting around each other every 3.45 days (Orosz et al. 2007). In the source LMC X-1, a $10.91 \pm 1.41 M_{\odot}$ BH orbits a $31.79 \pm 3.48 M_{\odot}$ O-star companion every 3.9 days (Orosz et al. 2009). These tight BH systems are expected to form from the primordial binaries that experienced either common envelope evolution (Orosz et al. 2007) or stable mass transfer (Valsecchi et al. 2010; Neijssel et al. 2021). There is a caveat that the accreting BHs are assumed to initially have negligible spins in our calculations, which seem to conflict with the ob-

served high BH spins in these known binaries (Fishbach & Kalogera 2021; see however Belczynski et al. 2021).

4. DISCUSSION

We demonstrate how to produce BBH mergers with a fast-spinning component by way of Case A mass transfer. Formation of such mergers requires close progenitor binaries with a massive companion around a BH. They directly result from close Wolf-Rayet star–O star binaries (van den Heuvel et al. 2017), who are widely observed in the Milky Way (van der Hucht 2001) and some nearby galaxies (e.g., Shenar et al. 2016, 2019). These systems are the evolutionary products of primordial binaries that experienced either a common envelope or a stable mass-transfer phase (e.g., Shao & Li 2016; Langer et al. 2020). A recent population synthesis study including all binary evolutionary stages indicated that the stable mass-transfer channel dominates the formation of local BBH mergers with large component masses

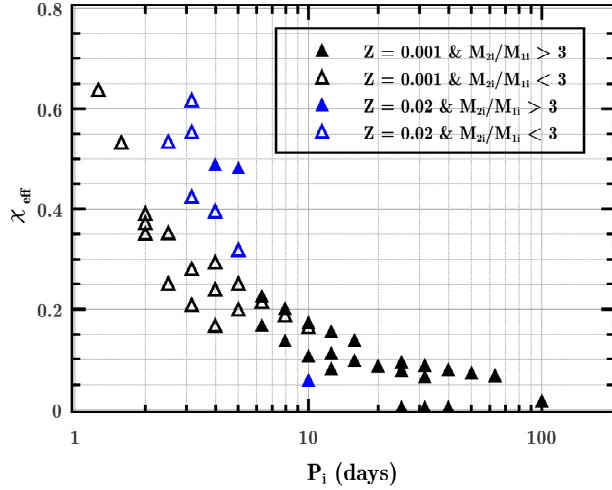


Figure 4. Relations between the effective spin parameters of calculated BBH mergers and the initial orbital periods of the progenitor binaries we evolved, by assuming that the BH accretion rate is limited by \dot{M}_{Edd} during the evolution. The open and filled triangles correspond to the progenitor systems with mass ratios (of the companion stars to the BHs) less than and larger than 3, respectively.

(van Son et al. 2021). Our work emphasizes that stable mass transfer from a massive donor to a BH accretor is not only an important pathway for the formation of BBH mergers, but also likely responsible for the origin of the high spins of the binaries.

ACKNOWLEDGMENTS

We thank the anonymous referee for constructive suggestions that helped improve this paper. This work was supported by the Natural Science Foundation of China (Nos. 11973026, 12121003, 12041301 and U1838201), and the National Program on Key Research and Development Project (Grant No. 2021YFA0718500).

REFERENCES

- Abbott, B. P., Abbott, R., Abbott, T. D., et al. 2016, *Phys. Rev. Lett.*, 116, 061102
- Abbott, B. P., Abbott, R., Abbott, T. D., et al. 2019, *Phys. Rev. X*, 9, 031040
- Abbott, R., Abbott, T. D., Abraham, S., et al. 2021a, *Phys. Rev. X*, 11, 021053
- Abbott, R., Abbott, T. D., Acernese, F., et al. 2021b, arxiv: 2111.03634
- Antonini, F., & Rasio, F. A. 2016, *ApJ*, 831, 187
- Askar, A., Szkudlarek, M., Gondek-Rosińska, D., Giersz, M., & Bulik, T. 2017, *MNRAS*, 464, L36
- Bardeen, J. M. 1970, *Nature*, 226, 64
- Bavera, S. S., Fragos, T., Qin, Y., et al. 2020, *A&A*, 635, 97
- Bavera, S. S., Fragos, T., Zevin, M. et al. 2021, *A&A*, 647, 153
- Begelman, M., 2002, *ApJ*, 568, 97
- Belczynski, K., Holz, D. E., Bulik, T., & O’Shaughnessy, R., 2016, *Nature*, 534, 512
- Belczynski, K., Klencki, J., Fields, C. E., et al. 2020, *A&A*, 636, A104
- Belczynski, K., Done, C., & Lasota, J. -P. 2021, arXiv: 2111.09401
- Breivik, K., Coughlin, S., Zevin, M., et al. 2020, *ApJ*, 898, 71
- Broekgaarden, F. S., Berger, E., Stevenson, S., et al. 2021, arXiv: 2112.05763
- Callister, T. A., Haster, C.-J., Ng, K. K. Y., et al. 2021, *ApJL*, 922, L5
- de Mink, S. E., & Mandel, I. 2016, *MNRAS*, 460, 3545
- Di Carlo, U. N., Giacobbo, N., Mapelli, M., et al. 2019, *MNRAS*, 487, 2947
- Downing, J. M. B., Benacquista, M. J., Giersz, M., & Spurzem, R., 2010, *MNRAS*, 407, 1946
- Eldridge, J. J., & Stanway, E. R. 2016, *MNRAS*, 462, 3302
- Fishbach, M., & Kalogera, V. 2021, arXiv: 2111.02935
- Fragione, G., & Loeb, A. 2019, *MNRAS*, 490, 4991
- Fragos, T., & McClintock, J. E. 2015, *ApJ*, 800, 17
- Fuller, J., & Lu, W. 2022, *MNRAS*, 511, 3951
- Galadage, S., Talbot, C., Nagar, T., et al. 2021, *ApJL*, 921, L15
- Gallegos-Garcia, M., Berry, C. P. L., Marchant, P., & Kalogera, V. 2021, *ApJ*, 922, 110
- Giacobbo, N., & Mapelli, M. 2018, *MNRAS*, 480, 2011
- Hoang, B.-M., Naoz, S., Kocsis, B., Rasio, F. A., & Dosopoulou, F. 2018, *ApJ*, 856, 140
- Khokhlov, S. A., Miroshnichenko, A. S., Zharikov, S. V., et al. 2018, *ApJ*, 856, 158
- King, A. R., & Kolb, U. 1999, *MNRAS*, 305, 654

- Kinugawa, T., Inayoshi, K., Hotokezaka, K., Nakauchi, D., & Nakamura, T. 2014, *MNRAS*, 442, 2963
- Kremer, K., Ye, C. S., Rui, N. Z., et al. 2020, *ApJS*, 247, 48
- Kruckow, M. U., Tauris, T. M., Langer, N., Kramer, M., & Izzard, R. G. 2018, *MNRAS*, 481, 1908
- Langer, N., Schürmann, C., Stoll, K. et al. 2020, *A&A*, 638, 39
- Lipunov, V. M., Postnov, K. A., & Prokhorov, M. E. 1997, *Astronomy Letters*, 23, 492
- Liu, B. & Lai, D. 2018, *ApJ*, 863, 68
- Mandel, I., & de Mink, S. E. 2016, *MNRAS*, 458, 2634
- Mandel, I., & Broekgaarden, F. S. 2022, *Living Rev Relativ*, 25, 1
- Mapelli, M., & Giacobbo, N. 2018, *MNRAS*, 479, 4391
- Mapelli, M., Bouffanais, Y., Santoliquido, F., et al. 2022, *MNRAS*, 511, 5797
- Marchant, P., Langer, N., Podsiadlowski, P., Tauris, T. M., & Moriya, T. J. 2016, *A&A*, 588, A50
- McKernan, B., Ford, K. E. S., Bellovary, J., et al. 2018, *ApJ*, 866, 66
- Miller-Jones, J. C. A., Bahramian, A., Orosz, Jerome A., et al. 2021, *Science*, 371, 1046
- Neijssel, C. J., Vigna-Gómez, A., Stevenson, S., et al. 2019, *MNRAS*, 490, 3740
- Neijssel, C. J., Vinciguerra, S., Vigna-Gómez, A., et al. 2021, *ApJ*, 908, 118
- Nitz, A. H., Kumar, S., Wang, Y.-F., et al. 2021, arXiv: 2112.06878
- Olejak, A., Belczynski, K., & Ivanova, N. 2021, *A&A*, 651, 100
- Olejak, A., & Belczynski, K. 2021, *ApJL*, 921, L2
- Orosz, J. A., McClintock, J. E., Narayan, R., et al. 2007, *Nature*, 449, 872
- Orosz, J. A., Steeghs, D., McClintock, J. E., et al. 2009, *ApJ*, 697, 573
- Paxton, B., Bildsten, L., Dotter, A., et al. 2011, *ApJS*, 192, 3
- Paxton, B., Cantiello, M., Arras, P., et al. 2013, *ApJS*, 208, 4
- Paxton, B., Marchant, P., Schwab, J., et al. 2015, *ApJS*, 220, 15
- Paxton, B., Schwab, J., Bauer, E. B., et al. 2018, *ApJS*, 234, 34
- Paxton, B., Smolec, R., Schwab, J., et al. 2019, *ApJS*, 243, 10
- Perna, R., Wang, Y.-H., Farr, W. M., Leigh, N., & Cantiello, M. 2019, *ApJ*, 878, L1
- Peters, P. C. 1964, *PhRv*, 136, 1224
- Podsiadlowski, P., Rappaport, S., & Han, Z. 2003, *MNRAS*, 341, 385
- Pols, O. R. 1994, *A&A*, 290, 119
- Qin, Y., Fragos, T., Meynet, G., et al. 2018, *A&A*, 616, 28
- Rappaport, S., Podsiadlowski, Ph., & Pfahl, E. 2005, *MNRAS*, 356, 401
- Rastello, S., Mapelli, M., Di Carlo, U. N., et al. 2020, *MNRAS*, 497, 1563
- Rodriguez, C. L., Haster, C.-J., Chatterjee, S., Kalogera, V., & Rasio, F. A. 2016, *ApJ*, 824, L8
- Roulet, J., Chia, H. S., Olsen, S., et al. *PhRvD*, 2021, 104, 083010
- Ruszkowski, M., & Begelman, M. C., 2003, *ApJ*, 586, 384
- Santoliquido, F., Mapelli, M., Bouffanais Y., et al. 2020, *ApJ*, 898, 152
- Shao, Y., & Li, X.-D. 2014, *ApJ*, 796, 37
- Shao, Y., & Li, X.-D. 2016, *ApJ*, 833, 108
- Shao, Y., & Li, X.-D. 2020, *ApJ*, 898, 143
- Shao, Y., & Li, X.-D. 2021, *ApJ*, 920, 81
- Shenar, T., Hainich, R., Todt, H., et al. 2016, *A&A*, 591, A22
- Shenar, T., Sablowski, D. P., Hainich, R., et al. 2019, *A&A*, 627, 151
- Silber, K., & Tremaine, S. 2017, *ApJ*, 836, 39
- Spera, M., Mapelli, M., Giacobbo, N., et al. 2019, *MNRAS*, 485, 889
- Stevenson, S., Vigna-Gómez, A., Mandel, I., et al. 2017, *Nature Communications*, 8, 14906
- Stevenson, S. 2022, *ApJ*, 926, L32
- Stone, N. C., Metzger, B. D., & Haiman, Z. 2017, *MNRAS*, 464, 946
- Tanikawa, A., Susa, H., Yoshida, T., Trani, A. A., & Kinugawa, T. 2021, *ApJ*, 910, 30
- Thorne, K. S. 1974, *ApJ*, 191, 507
- Tutukov, A. V. & Yungelson, L. R. 1993, *MNRAS*, 260, 675
- Valsecchi, F., Glebbeek, E., Farr, Will M., et al. 2010, *Nature*, 468, 77
- van den Heuvel, E. P. J., Portegies Zwart, S. F., & de Mink, S. E. 2017, *MNRAS*, 471, 4256
- van der Hucht, K. A. 2001, *NewAR*, 45, 135
- van Son, L. A. C., de Mink, S. E., Broekgaarden, F. S., et al. 2020, *ApJ*, 897, 100
- van Son, L. A. C., de Mink, S. E., Callister, T., et al. 2021, arXiv: 2110.01634
- Voss, R. & Tauris, T. M. 2003, *MNRAS*, 342, 1169
- Wellstein, S., Langer, N., & Braun, H. 2001, *A&A*, 369, 939
- Zevin, M., Spera, M., Berry, C. P. L., & Kalogera, V. 2020, *ApJ*, 899, L1
- Zevin, M., & Bavera, S. S. 2022, arXiv: 2203.02515
- Ziosi, B. M., Mapelli, M., Branchesi, M., & Tormen, G. 2014, *MNRAS*, 441, 3703